第 34 卷第 8 期
2018 年 8 月

无 机 化 学 学 报
CHINESE JOURNAL OF INORGANIC CHEMISTRY

Vol.34 No.8
1547-1554

具有缓慢磁弛豫行为的单核 Dy(Ⅲ)和 Ho(Ⅲ)配合物

李东平*,[1] 王 倩[1] 谢一步[1] 张 俊[2] 连庆云[1] 李永绣*,[1]

([1]南昌大学化学系,南昌 330031)

([2]安徽建筑大学功能分子设计与界面过程重点实验室,合肥 230022)

摘要:以席夫碱配体 *N*,*N*′-双(3-甲氧基亚水杨基)乙烯-1,2-二胺(H_2salen)为原料,合成了 2 个新的镧系配合物,即$[Dy(salen)_2]_3\cdot 3C_2H_9N_2\cdot 2CH_3OH$ (**1**),$[Ho(salen)_2]_3\cdot 3C_2H_9N_2\cdot 1.5CH_3OH$ (**2**),并对其进行了基本表征。X 射线单晶衍射结果表明,配合物 **1** 和 **2** 结晶于单斜晶系 *C*2 空间群,其金属配位环境类似。配合物 **1** 和 **2** 在零场和外加磁场下均具有单分子磁体(SMMs)行为。

关键词:镧系配合物;晶体结构;单分子磁体

中图分类号:O614.342;O614.343 **文献标识码**:A **文章编号**:1001-4861(2018)08-1547-08

DOI:10.11862/CJIC.2018.170

Mononuclear Dy(Ⅲ) and Ho(Ⅲ) Complexes with Slow Magnetic Relaxation Behavior

LI Dong-Ping*,[1] WANG Qian[1] XIE Yi-Bu[1] ZHANG Jun[2] LIAN Qing-Yun[1] LI Yong-Xiu*,[1]

([1]*Department of Chemistry, Nanchang University, Nanchang* 330031, *China*)

([2]*Key Laboratory of Functional Molecule Design and Interface Process, Anhui Jianzhu University, Hefei* 230022, *China*)

Abstract: Two new lanthanide complexes based on Schiff base ligand, namely $[Dy(salen)_2]_3\cdot 3C_2H_9N_2\cdot 2CH_3OH$ (**1**) and $[Ho(salen)_2]_3\cdot 3C_2H_9N_2\cdot 1.5CH_3OH$ (**2**), (H_2salen=*N*,*N*′-bis(3-methoxysalicylidene)ethylene-1,2-diamine), have been synthesized and characterized. Single-crystal X-ray diffractions reveal that **1** and **2** crystallize in the same monoclinic space group *C*2, and have similar coordination environment around the metallic centers. Single molecule magnets (SMMs) behaviors have been observed in **1** and **2** with/without an applied magnetic field. CCDC: 1827419, **1**; 1827420, **2**.

Keywords: Lanthanide complex; crystal structure; single-molecule magnet

0 Introduction

Due to the significant magnetic anisotropy arising from the large unquenched orbital angular momentum, lanthanide ions, such as Tb(Ⅲ), Dy(Ⅲ), Ho(Ⅲ), Er(Ⅲ), are attractive metal centers for the design and synthesis of high-barrier SMMs with potential applications in high-density magnetic memories, quantum computing devices, and molecular spintronics[1-7]. A rapid growth in pure lanthanide SMMs with intriguing magnetic properties has been seen in recent years after the observation of slow magnetic relaxation in the cases of mononuclear complexes[8-9]. Among them, dysprosium(Ⅲ) based complexes present ideal candidates for SMMs because Dy(Ⅲ) is a Kramers ion combining a large-moment $^6H_{15/2}$ ground state with significant anisotropy of the 4*f* shell[10].

However, rational design and synthesis of lanthanide SMMs with high relaxation barrier is still a huge challenge. Generally, ligand is a key factor in

收稿日期:2018-03-08。收修改稿日期:2018-05-03。

国家自然科学基金(No.21101090,21561021)、江西省自然科学基金(No.20114BAB213001)和江西省教育厅项目(No.GJJ12041)资助。

*通信联系人。E-mail:nculdp@126.com,yxli@ncu.edu.cn

construction of SMMs, which influences the ligand-field and magnetic interaction in complex. Hence, lots of bridging ligands and multidentate ligands are synthesized to modulate the properties of lanthanide SMMs. Among them, Schiff bases and their complexes can be easily synthesized and modified, which have potential applications in fluorescent sensors, SMMs and molecular recognitions, *etc*[11-14]. For instance, salen-type complexes are of special interest due to their potential applications in catalysts, biological and magnetic materials[15-23]. It is worthy to notice that most of those salen-type complexes are 3*d* or 3*d*-4*f* compounds. Only a few pure lanthanide compounds are reported based on this ligand[24-27]. Herein, we report the synthesis, structure and magnetism of two eight-coordinate Ln(Ⅲ) complexes (Ln=Dy (**1**), Ho (**2**)) based on the H_2salen Schiff bases ligand. Complexes **1** and **2** showed SMMs behavior with/without an applied magnetic field.

1 Experimental

1.1 General methods

Reagents and solvents were purchased commercially and used as received. FT-IR spectra were recorded in KBr pellet on a vector 22 Bruker spectrophotometer in the range of 400~4 000 cm^{-1}. C, H and N microanalyses were performed on a Perkin-Elmer 240C analyzer. The powder XRD patterns were recorded on a Shimadzer at 40 kV, 30 mA using a Cu $K\alpha$ radiation (λ=0.154 06 nm) in 2θ range of 5°~50°. Thermal stability studies were performed on a Perkin-Elmer Pyris 1 TGA analyzer from room temperature to 800 ℃ with a heating rate of 20 ℃·min^{-1} under nitrogen. Susceptibility measurements and field dependence of magnetization on polycrystalline samples were performed on a Quantum Design MPMS-XL7 SQUID magnetometer.

1.2 Preparation

1.2.1 Synthesis of $[Dy(salen)_2]_3\cdot 3C_2H_9N_2\cdot 2CH_3OH$ (**1**)

A mixture of $Dy(NO_3)_3\cdot 6H_2O$ (0.1 mmol), *o*-vanillin (0.2 mmol) and ethylenediamine (0.4 mL) was dissolved in 20 mL methanol, and then stirred for 3 h. The resulting solution was filtrated and kept untouched at room temperature for one week. Yellow stick crystals were collected, washed with methanol and dried in air. Yield: 39.4% based on $Dy(NO_3)_3\cdot 6H_2O$. Anal. Calcd. for $C_{116}H_{143}Dy_3N_{18}O_{26}$(%): C, 51.74; H, 5.35; N, 9.36. Found(%): C, 51.86; H, 5.42; N, 9.41. IR: 2 905 (m), 1 623(s), 1 542(m), 1 449(s), 1 389(s), 1 310(s), 1 217(s), 1 164(w), 1 077(m), 971(m), 851(m), 784(w), 732(s), 632(w).

1.2.2 Synthesis of $[Ho(salen)_2]_3\cdot 3C_2H_9N_2\cdot 1.5CH_3OH$ (**2**)

Complex **2** was prepared similarly to complex **1**, but using $Ho(NO_3)_3\cdot 6H_2O$ instead of $Dy(NO_3)_3\cdot 6H_2O$, and $Ni(NO_3)_3\cdot 6H_2O$ (0.25 mmol) was also added in the solution. Yield: 30.4% based on $Ho(NO_3)_3\cdot 6H_2O$. Anal. Calcd. for $C_{115.5}H_{141}Ho_3N_{18}O_{25.5}$(%): C, 51.63; H, 5.25; N, 9.34. Found(%): C, 51.60; H, 5.22; N, 9.30. IR: 2 915(m), 1 627(s), 1 546(m), 1 450(s), 1 388(s), 1 320 (s), 1 224(s), 1 162(w), 1 079(m), 976(m), 853(m), 778 (w), 736(s), 640(w).

1.3 Crystal structure determination

Single-crystal X-ray diffraction data were collected on a Bruker D8 QUEST CCD diffractometer equipped with a graphite-monochromatic Mo $K\alpha$ radiation (λ=0.071 073 nm) by using an φ-ω scan mode at room temperature. The structures were solved by direct methods using the SHELXS-97[28], and refined by full-matrix least-squares on F^2[29]. All non-hydrogen atoms were refined anistropically. Hydrogen atoms were generated geometrically and refined isotropically with the riding mode. Details of crystal parameters, selected bond lengths and bond angles are given in Table 1 and 2, respectively.

CCDC: 1827419, **1**; 1827420, **2**.

2 Results and discussion

2.1 Crystal structure of the complexes

Single crystal structure analysis reveals that complexes **1** and **2** are isostructural and the X-ray structure of **1** is selectively described in the following discussion. Complex **1** crystallizes in monoclinic space group of *C*2. As shown in Fig.1a, the asymmetric unit of complex **1** contains three Schiff base ligands, one and a half Dy atom, two distorted methanol molecules,

Table 1　Crystal data of 1 and 2

	1	2
Empirical formula	$C_{116}H_{142}Dy_3N_{18}O_{26}$	$C_{115.5}H_{141}Ho_3N_{18}O_{25.5}$
Formula weight	2 691.97	2 684.24
Temperature / K	296(2)	296(2)
Crystal system	Monoclinic	Monoclinic
Space group	*C*2	*C*2
a / nm	1.932 74(11)	1.935 01(8)
b / nm	2.337 25(13)	2.338 37(10)
c / nm	1.434 06(8)	1.429 98(6)
β / (°)	107.457 0(10)	107.427 0(3)
Volume / nm^3	6.179 7(6)	6.173 3(4)
Z	2	2
D_c / ($g\cdot cm^{-3}$)	1.447	1.444
F(000)	2 740	2 730
Limiting indices	$-20 \leqslant h \leqslant 25, -30 \leqslant k \leqslant 31, -19 \leqslant l \leqslant 19$	$-23 \leqslant h \leqslant 23, -28 \leqslant k \leqslant 28, -17 \leqslant l \leqslant 17$
Reflection collected	13 431	10 539
Final *R* indices	R_1=0.042 7, wR_2^a=0.113 3	R_1=0.032 4, wR_2^a=0.090 4
R indices(all data)	R_1=0.048 3, wR_2^a=0.118 9	R_1=0.033 89, wR_2^a=0.091 3
Goodness-of-fit on F^2	1.154	1.143

[a] $w=1/[\sigma^2(F_o^2)+(0.061\ 6P)^2+14.148\ 1P]$ where $P=(F_o^2+2F_c^2)/3$ for **1**; $w=1/[\sigma^2(F_o^2)+(0.064\ 5P)^2]$ where $P=(F_o^2+2F_c^2)/3$ for **2**.

Table 2　Selected bond lengths (nm) and bond angles (°) for 1 and 2

1					
Dy(2)-O(2)	0.231 2(6)	Dy(1)-O(10)	0.229 3(5)	Dy(2)-N(3)	0.255 4(7)
Dy(2)-O(3)	0.227 6(6)	Dy(1)-O(11)	0.230 4(6)	Dy(2)-N(4)	0.250 8(5)
Dy(2)-O(6)	0.231 7(6)	Dy(2)-N(1)	0.254 6(8)	Dy(1)-N(5)	0.252 4(5)
Dy(2)-O(7)	0.228 7(5)	Dy(2)-N(2)	0.253 2(8)	Dy(1)-N(6)	0.256 2(7)
O(10)-Dy(1)-O(10^i)	78.09	O(11)-Dy(1)-O(11^i)	132.12	O(7)-Dy(2)-O(2)	148.13
O(10)-Dy(1)-O(11)	80.38	O(3)-Dy(2)-O(2)	79.98	O(7)-Dy(2)-O(6)	80.13
O(10)-Dy(1)-O(11^i)	142.92	O(3)-Dy(2)-O(6)	148.82	O(3)-Dy(2)-O(7)	80.21
2					
Ho(1)-O(2)	0.229 8(5)	Ho(2)-O(10)	0.228 9(6)	Ho(1)-N(3)	0.249 3(7)
Ho(1)-O(3)	0.225 9(6)	Ho(2)-O(11)	0.227 7(5)	Ho(1)-N(4)	0.253 7(8)
Ho(1)-O(6)	0.227 4(6)	Ho(1)-N(1)	0.252 0(9)	Ho(2)-N(5)	0.249 6(7)
Ho(1)-O(7)	0.230 0(5)	Ho(1)-N(2)	0.251 8(9)	Ho(2)-N(6)	0.253 3(7)
O(10)-Ho(2)-O(10^i)	78.83	O(3)-Ho(1)-O(2)	79.89	O(3)-Ho(1)-O(7)	148.72
O(11)-Ho(2)-O(10)	143.02	O(11)-Ho(2)-O(11^i)	132.13	O(6)-Ho(1)-O(2)	148.12
O(11)-Ho(2)-O(10)	80.12	O(3)-Ho(1)-O(6)	80.14	O(6)-Ho(1)-O(7)	80.32

Symmetry codes: [i] $1-x, y, 1-z$ for **1**; [i] $-x, y, -z$ for **2**.

one and a half protonated ethylenediamine molecules. Each Dy atom is eight-coordinated by four imine-N atoms and four hydroxyl-O atoms from two distinct $salen^{2-}$ ligands, forming a sandwich structure. It is interesting there are two different coordination parts in an asymmetric unit. Unlike those reported Ln-salen-type complexes[7], the methoxy-O atoms in Schiff base ligand are not coordinated with lanthanide ions. The

average Dy-O bond lengths is 0.229 8 nm (range from 0.229 3(5) to 0.230 4(6) nm), which is shorter than the average Dy-N bond lengths (0.253 8 nm, range from 0.250 8(5) to 0.256 2(7) nm) in molecule. The intramolecular Dy(1)···Dy(2) distance is 0.946 3 nm.

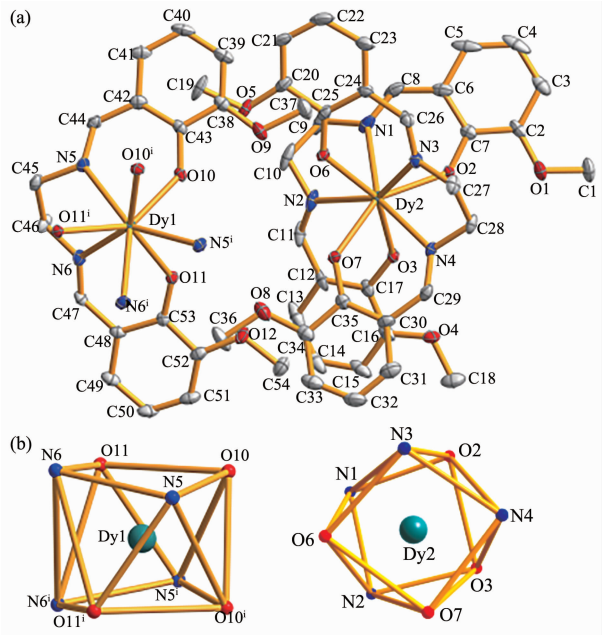

Hydrogen atoms are omitted for clarity; Symmetry codes: [i] 1−*x*, *y*, 1−*z*

Fig.1 (a) Coordination environment of the Dy(Ⅲ) ions and the labeling scheme with 30% ellipsoidal prohability; (b) Distorted square antiprism geometry of Dy(Ⅲ) ion in the complex

The coordination geometry of the Dy(Ⅲ) ion can be described as a distorted square antiprism (Fig.1b). The O(10), O(11), N(5), N(6) and O(10^{i}), O(11^{i}), N(5^{i}), N(6^{i}) atoms form the bottom and top planes of square antiprism in Dy(1) unit with mean deviations of 0.016 6 and 0.056 6 nm, respectively. The O(2), O(3), N(1), N(2) and O(6), O(7), N(3), N(4) atoms form other two planes of square antiprism in Dy(2) unit with mean deviations of 0.066 5 and 0.041 4 nm. The dihedral angles of the two planes in distinct square antiprism are 4.43° and 5.68°, respectively.

As illustrated in Fig.2, there are abundant intramolecular hydrogen-bonding interactions between hydroxyl or methoxy groups of ligands and protonated ethylenediamine molecules. The adjacent Dy(1) molecules are interconnected by hydrogen bonds with the Dy(2) molecules, forming an infinite Dy(1)···Dy(2)···Dy(2)···Dy(1) chain. The D···A distances and D−H···A angles of hydrogen bonds range from 0.274 1 to 0.300 9 nm and 132.71° to 150.33°, respectively (Table 3).

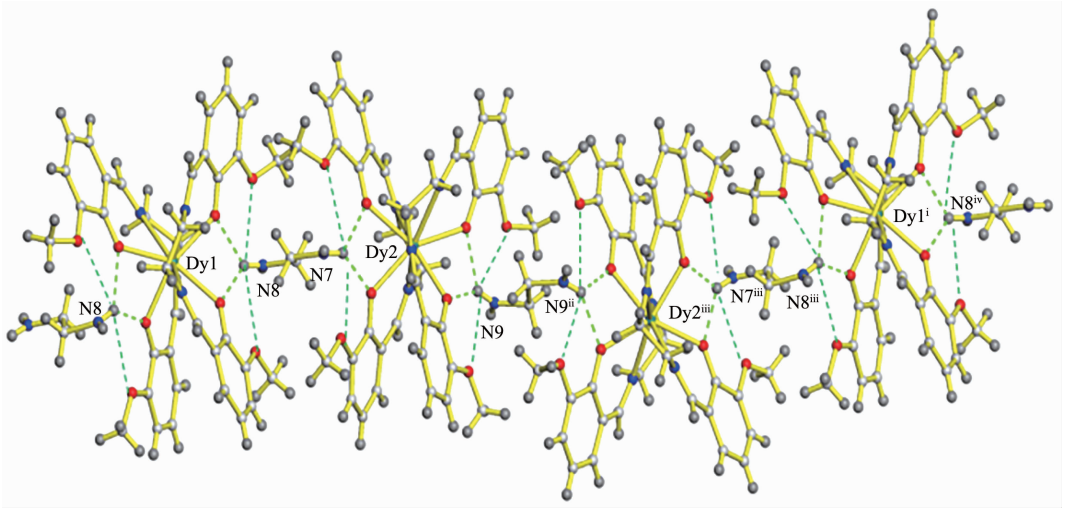

Symmetry codes: [i] 1−x, y, 1−z; [ii] x, y, −1+z; [iii] 2−x, y, −z; [iv] 1+x, y, −1+z

Fig.2 One dimensional chain formed by hydrogen bonds

Table 3 Hydrogen-bonding geometry parameters for 1 and 2

D−H···A	*d*(D-H) / nm	*d*(H···A) / nm	*d*(D···A) / nm	∠DHA / (°)
		1		
N(8)−H(8A)···O(9)	0.089 1	0.223 7(5)	0.291 6(4)	132.71(6)
N(8)−H(8A)···O(10)	0.089 1	0.195 4(7)	0.276 4(6)	150.33(6)

Continued Table 3

N(8)–H(8C)···O(11)	0.088 9	0.200 8(8)	0.276 0(5)	141.51(3)
N(8)–H(8C) ···O(12)	0.088 9	0.224 2(4)	0.300 9(4)	141.43(5)
N(9)–H(9C)···O(1^{ii})	0.089 0	0.223 3(3)	0.293 3(4)	136.57(5)
N(9)–H(9C)···O(2^{ii})	0.089 0	0.296 1(4)	0.274 1(5)	145.84(4)
N(9)–H(9E)···O(3^{ii})	0.089 1	0.198 6(6)	0.274 9(6)	142.82(8)
N(9)–H(9E)···O(4^{ii})	0.089 1	0.218 6(7)	0.289 1(5)	137.74(6)
		2		
N(8)–H(8A)···O(9^{i})	0.088 9	0.225 9	0.288 2	126.86(9)
N(8)–H(8A)···O(10^{i})	0.089 1	0.191 2	0.274 6	155.42(8)
N(8)–H(8C)···O(11^{ii})	0.089 0	0.205 0	0.275 5	135.51(6)
N(8)–H(8C)···O(12^{ii})	0.089 0	0.221 9	0.299 5	145.66(7)
N(9)–H(9C)···O(1^{iii})	0.089 0	0.231 0	0.291 4	131.78(2)
N(9)–H(9C)···O(2^{iii})	0.089 0	0.194 0	0.274 3	153.17(4)
N(9)–H(9D)···O(3^{iii})	0.089 0	0.210 1	0.275 5	135.72(1)
N(9)–H(9E)···O(4^{iii})	0.089 1	0.210 3	0.288 3	143.72(9)

Symmetry codes: ^{ii} x, y, z+1 for **1**; ^{i} –x, y, 1–z; ^{ii} x, y, 1+z; ^{iii} 1–x, y, 1–z for **2**.

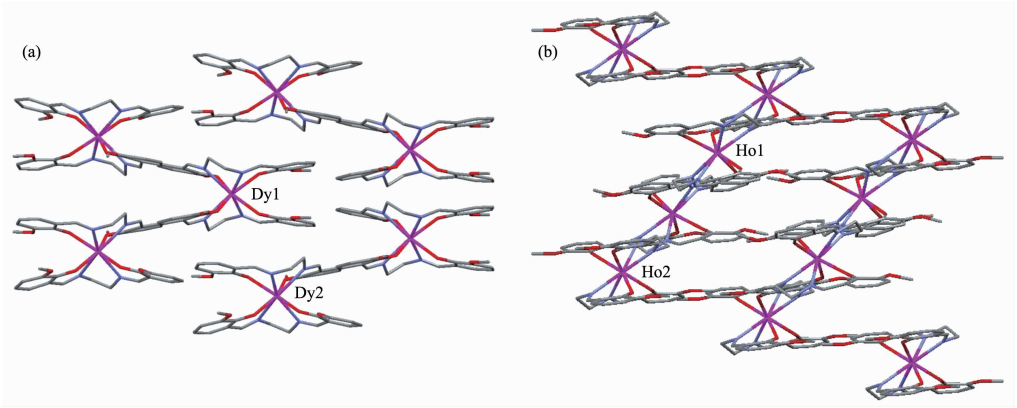

Fig.3　Packing diagrams of complexes **1** (a) and **2** (b)

Complex **2** is isostructural with that of **1**. However, it is interesting that the two complexes show different packing diagrams in a cell volume (Fig.3). This may be due to the changes in quantity and location of lattice molecules, especially the methanol molecules in complexes.

2.2　Powder X-ray diffraction

Isostructural complexes with different packing diagrams are less reported. To confirm the phase purity and exactness of the crystal structures of the complexes, X-ray powder diffraction (PXRD) analyses were performed on single crystal samples at room temperature. As illustrated in Fig.4, the X-ray powder diffraction patterns of **1** and **2** are in agreement with the simulated one from the single-crystal X-ray data. It suggests that complexes **1** and **2** are isostructural, and the crystal structures are truly representative of the bulk material.

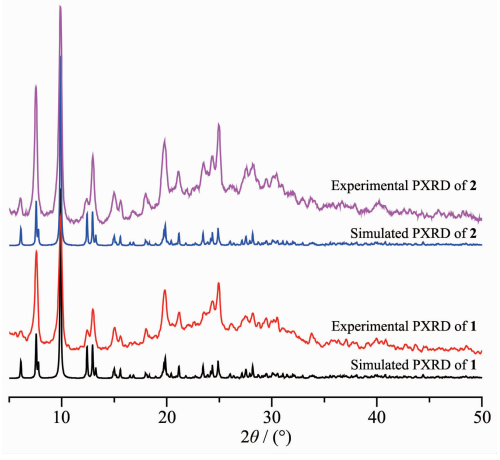

Fig.4　Powder X-ray diffraction patterns of **1** and **2**

2.3 Magnetic properties

The variable temperature magnetic susceptibility measurements of **1** and **2** were performed on polycrystalline samples in the temperature range of 1.8~300 K under an external dc field of 2 kOe (Fig.5). At room temperature, the $\chi_m T$ values are 14.18 emu·K·mol^{-1} for **1** and 13.92 emu·K·mol^{-1} for **2**, which are close to the expected value for one paramagnetic Dy(Ⅲ) (14.17 emu·K·mol^{-1}, J=15/2, g=4/3) and Ho(Ⅲ) ions (14.06 emu·K·mol^{-1}, J=8, g=5/4). Upon cooling, the $\chi_m T$ for **1** gradually decrease until 50 K and then quickly decrease to the corresponding values of 7.82 emu·K·mol^{-1} at 1.8 K, while the $\chi_m T$ for **2** decrease quickly after 100 K to reach a minimum of 6.20 emu·K·mol^{-1} at 1.8 K.

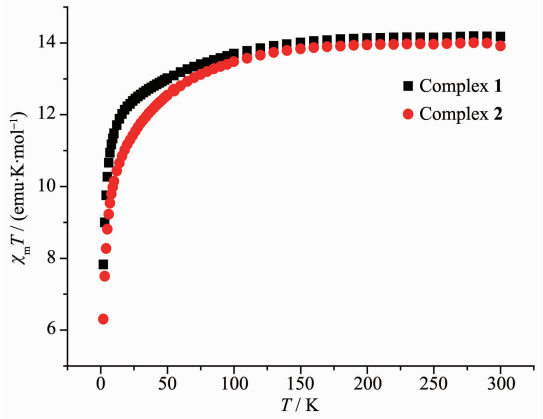

Fig.5 Plots of $\chi_m T$ versus T in a dc field of 2 kOe for **1** and **2**

The dynamics of the magnetization of **1** and **2** were investigated using alternating-current (ac) magnetic susceptibility measurements at ac field strength of 3.0 kOe with/without an applied dc field. The results reveal that complexes **1** and **2** show some possible features associated with slow magnetization relaxation of SMMs with/without an applied 2 kOe dc field (Fig.6~7). As shown in Fig.6a and 6b, the out-of-phase (χ'') signals of **1** show weak frequency dependence at low temperature. To elucidate the details of the relaxation dynamics, a static field of 2 kOe was applied in ac measurements to reduce the quantum tunnelling at low temperature region of **1**. As exhibited in Fig.6c and 6d, the frequency dependence of the ac susceptibility is observed more clearly under an

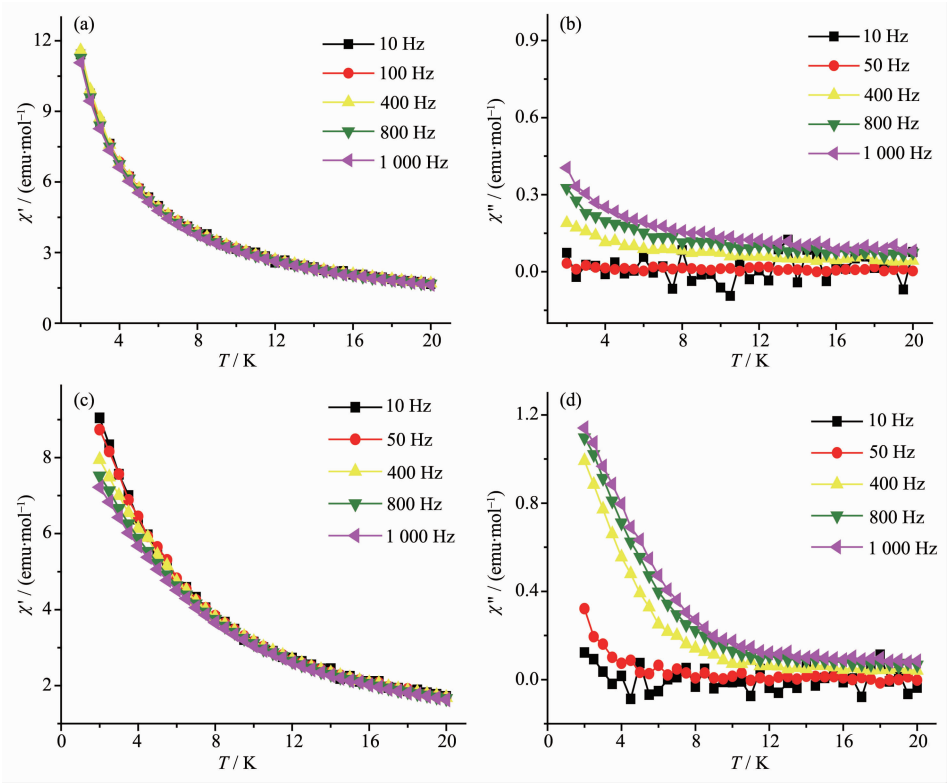

(a, b) under a zero dc field; (c, d) under a dc field of 2 kOe

Fig.6 Temperature dependence of the in-phase (a, c) and out-of-phase (b, d) dynamic susceptibility of **1** at ac magnetic field of 3 kOe

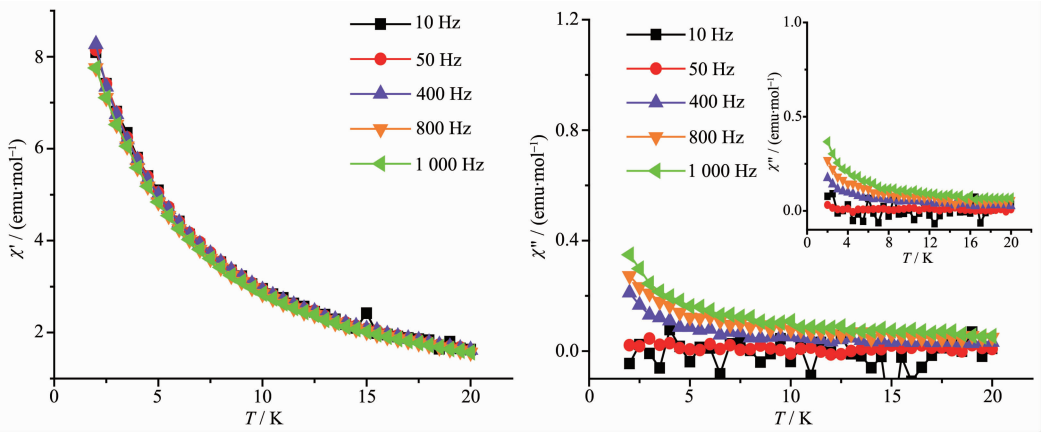

Inset: Out-of-phase dynamic susceptibility of **2** under a zero dc field

Fig.7 Temperature dependence of the in-phase and out-of-phase dynamic susceptibility of **2** under a dc field of 2 kOe

external dc field. Both the in-phase (χ') and out-of-phase (χ'') signals of **1** show frequency dependence behaviors at low temperature, but no frequency dependent peaks were observed. Hence, the corresponding energy barrier of **1** can′t be fitted with the Arrhenius law. However, the slow magnetic relaxation behavior of **1** indicates that the complex may be a SMM. The χ'' signal of **2** also shows possible frequency depe ndence at low temperature with or without an external dc field (Fig.7). However, no frequency dependence behaviors were observed in the in-phase signals of compound. Furthermore, the out-of-phase signal of **2** doesn′t exhibit obvious changes under an applied field. The result indicates there is strong quantum tunnelling in the low temperature region of **2**.

3 Conclusions

Two isostructural lanthanide (Dy and Ho) complexes were synthesized in two synthetic approaches. Detailed magnetic study reveals that the lanthanide-salen type compounds with sandwich structure show SMMs behavior, which indicates complex **1** may be a single molecular magnet.

References:

[1] Liu S S, Meng Y S, Gao S, et al. *Inorg. Chem.*, **2017**,**56**(13): 7320-7323

[2] YANG Yu-Ting(杨玉亭), TU Chang-Zheng(屠长征), YAO Li-Feng(姚立峰), et al. *Chinese J. Inorg. Chem.*(无机化学学报), **2016**,**32**(8):1311-1318

[3] Gregson M, Chilton N F, Ariciu A M, et al. *Chem. Sci.*, **2016**,**7**(1):155-165

[4] Peng J B, Zhang Q C, Kong X J, et al. *J. Am. Chem. Soc.*, **2012**,**134**(7):3314-3317

[5] Liu J L, Yuan K, Leng J D, et al. *Inorg. Chem.*, **2012**,**51**(15): 8538-8544

[6] Magnani N, Apostolidis C, Morgenstern A, et al. *Angew. Chem. Int. Ed.*, **2011**,**50**(7):1696-1698

[7] Craig G A, Murrie M. *Chem. Soc. Rev.*, **2015**,**44**(8):2135-2147

[8] Ishikawa N, Sugita M, Ishikawa T, et al. *J. Am. Chem. Soc.*, **2003**,**125**(29):8694-8695

[9] Das C, Upadhyay A, Vaidya S, et al. *Chem. Commun.*, **2015**, **51**(28):6137-6140

[10]Akhtar M N, Liao X F, Chen Y C, et al. *Dalton Trans.*, **2017**,**46**(9):2981-2987

[11]Rinehart J D, Meihaus K R, Long J R. *J. Am. Chem. Soc.*, **2010**,**132**(22):7572-7573

[12]Blagg R J, Muryn C A, McInnes E J L, et al. *Angew. Chem. Int. Ed.*, **2011**,**50**(29):6530-6533

[13]Blagg R J, Ungur L, Tuna F, et al. *Nat. Chem.*, **2013**,**5**(8): 673-678

[14]Woodruff D N, Winpenny R E P, Layfield R A. *Chem. Rev.*, **2013**,**113**(7): 5110-5148

[15]Adão P, Barroso S, Avecilla F, et al. *J. Organomet. Chem.*, **2014**,**760**:212-223

[16]Roy S, Drew M G B, Bauzá A, et al. *CrystEngComm*, **2018**, **20**(12):1679-1689

[17]Kaczmarek A M, Porebski P W A, Mortier T, et al. *J. Inorg. Biochem.*, **2016**,**163**:194-205

[18]ZOU Xiao-Yan(邹晓艳), MA Hui-Yuan(马慧媛), PANG

Hai-Jun(庞海军), et al. *Chinese J. Inorg. Chem.*(无机化学学报), **2016**,**32**(9):1647-1652

[19]Andruh M. *Dalton Trans.*, **2015**,**44**(38):16633-16653

[20]Leuenberger M N, Loss D. *Nature*, **2001**,**410**(6830):789-793

[21]Bogani L, Wernsdorfer W. *Nat. Mater.*, **2008**,**7**(3):179-186

[22]Mannini M, Pineider F, Sainctavit P, et al. *Nat. Mater.*, **2009**,**8**(3):194-197

[23]Ganzhorn M, Klyatskaya S, Ruben M, et al. *Nat. Nanotechnol.*, **2013**,**8**(3):165-169

[24]Chen Y C, Liu J L, Ungur L, et al. *J. Am. Chem. Soc.*, **2016**,**138**(8):2829-2837

[25]Xia H T, Liu Y F, Ma W X. *J. Coord. Chem.*, **2013**,**66**(21):3706-3721

[26]Costes J P, Laussac J P, Nicodème F. *J. Chem. Soc. Dalton Trans.*, **2002**(13):2731-2736

[27]LIU Jian(刘建), ZHANG Xiao-Peng(张小朋), LI Cheng-Hui(李承辉). *Chinese J. Inorg. Chem.*(无机化学学报), **2017**,**33**(11):2060-2064

[28]Sheldrick G M. *SHELXS*-97, *Program for the Solution of Crystal Structures*, University of Göttingen, Germany, **1997**.

[29]Sheldrick G M. *SHELXL*-97, *Program for the Refinement of Crystal Structures*, University of Göttingen, Germany, **1997**.